

Electronic Structure of the Alkyne-Bridged Dicobalt Hexacarbonyl Complex $\text{Co}_2 \mu\text{-C}_2\text{H}_2 (\text{CO})_6$: Evidence for Singlet Diradical Character and Implications for Metal–Metal Bonding

James A. Platts,*† Gareth J. S. Evans,† Michael P. Coogan,† and Jacob Overgaard‡

School of Chemistry, Cardiff University, Park Place, Cardiff CF10 3AT, U.K., and Department of Chemistry, University of Aarhus, Langelandsgade 140, DK-8000 Aarhus C, Denmark

Received February 12, 2007

A series of ab initio calculations are presented on the alkyne-bridged dicobalt hexacarbonyl cluster $\text{Co}_2 \mu\text{-C}_2\text{H}_2 (\text{CO})_6$, indicating that this compound has substantial multireference character, which we interpret as evidence of singlet diradical behavior. As a result, standard theoretical methods such as restricted Hartree–Fock (RHF) or Kohn–Sham (RKS) density functional theory cannot properly describe this compound. We have therefore used complete active space (CAS) methods to explore the bonding in and spectroscopic properties of $\text{Co}_2 \mu\text{-C}_2\text{H}_2 (\text{CO})_6$. CAS methods identify significant population of a Co–Co antibonding orbital, along with Co– π^* back-bonding, and a relatively large singlet–triplet energy splitting. Analysis of the electron density and related quantities, such as energy densities and atomic overlaps, indicates a small but significant amount of covalent bonding between cobalt centers.

Introduction

The electronic structure of and bonding within transition metal clusters has long been the center of experimental¹ and theoretical² attention. In such studies, analysis of electron density within the framework of Bader’s quantum theory of atoms in molecules (QTAIM)³ has proven to be especially useful, allowing orbital-independent comparison between

experiment and theory. Recent theoretical studies suggest that the electron density alone may be insufficient to reveal the fine detail of the region between bridged metal atoms, and this region is found to be characteristically flat for experimental densities.^{1c,e} Instead, the total electronic energy density, $H(\mathbf{r})$, has been proposed as an alternative to the electron density. This follows the pioneering work by Cremer and Kraka⁴ on the description of chemical bonding using the kinetic ($G(\mathbf{r})$) and potential ($V(\mathbf{r})$) energy densities.

Numerous studies have employed the prototypical cobalt dimer, $\text{Co}_2(\text{CO})_8$, a fluxional molecule which contains two bridging carbonyl groups in its lowest-energy form, to study metal–metal bonding. On the basis of orbital symmetry arguments, Thorn and Hoffmann suggest the presence of a bent metal–metal bond.⁵ Leung & Coppens^{1a} studied the experimental electron density of this compound, finding no evidence for density accumulation in the Co–Co region to reflect bonding (bent or straight) between the Co atoms. Topological analysis of the theoretical electron density showed (3, –1) bond critical points (bcp) only in the Co–C bonds, while a (3, +1) ring critical point (rcp) was found close to the Co–Co midpoint, apparently at variance with the prediction of a Co–Co single bond and the observation

*To whom correspondence should be addressed. E-mail: platts@cf.ac.uk.

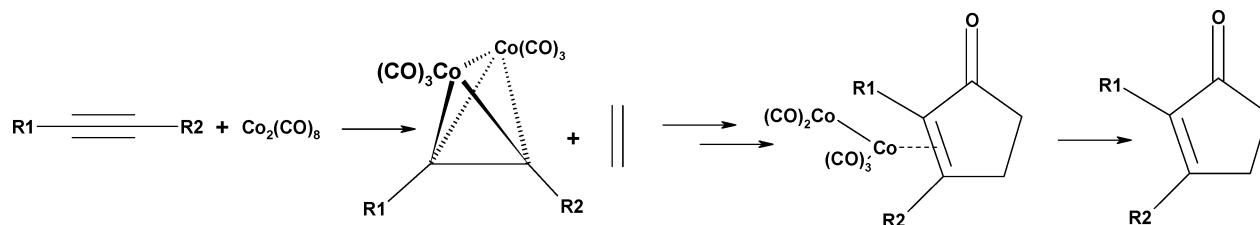
† Cardiff University.

‡ University of Aarhus.

- (1) (a) Leung, P.; Coppens, P. *Acta Crystallogr., Sect. B* **1983**, *39*, 535. (b) Bianchi, R.; Gervasio, G.; Marabello, D. *Acta Crystallogr., Sect. B* **2001**, *57*, 638. (c) Bianchi, R.; Gervasio, G.; Marabello, D. *Helv. Chim. Acta* **2001**, *84*, 722. (d) Bianchi, R.; Gervasio, G.; Marabello, D. *Chem. Commun.* **1998**, 1535. (e) Bianchi, R.; Gervasio, G.; Marabello, D. *Inorg. Chem.* **2000**, *39*, 2360. (f) Macchi, P.; Proserpio, D. M.; Sironi, A. *J. Am. Chem. Soc.* **1998**, *120*, 13429. (g) Macchi, P.; Garlaschelli, L.; Martinengo, S.; Sironi, A. *J. Am. Chem. Soc.* **1999**, *121*, 10428. (h) Farrugia, L. J.; Mallinson, P. R.; Stewart, B. *Acta Crystallogr., Sect. B* **2003**, *59*, 234.
- (2) (a) Low, A. A.; Kunze, K. L.; MacDougall, P. J.; Hall, M. B. *Inorg. Chem.* **1991**, *30*, 1079–1086. (b) Low, A. A.; Hall, M. B. *Inorg. Chem.* **1993**, *32*, 3880–3889. (c) Bo, C.; Sarasa, J.-P.; Poblet, J.-M. *J. Phys. Chem.* **1993**, *97*, 6362–6366. (d) Finger, M.; Reinhold, J. *Inorg. Chem.* **2003**, *42*, 8128–8130. (e) Kluge, O.; Finger, M.; Reinhold, J. *Inorg. Chem.* **2005**, *44*, 6494. (f) Roos, B. O.; Borin, A. C.; Gagliardi, L. *Angew. Chem., Int. Ed.* **2007**, *46*, 1469. (g) Frenking, G.; Tonner, R. *Nature* **2007**, *446*, 276.
- (3) (a) Bader, R. F. W. *Atoms in Molecules—A Quantum Theory*; Cambridge University Press: Oxford, U.K., 1990. (b) Popelier, P. L. A. *Atoms in Molecules: An Introduction*; Harlow: New York, 2000.

(4) (a) Cremer, D.; Kraka, E. *Angew. Chem., Int. Ed.* **1984**, *23*, 627. (b) Cremer, D.; Kraka, E. *Croat. Chem. Acta* **1984**, *57*, 1259.

(5) Thorn, D. L.; Hoffmann, R. *Inorg. Chem.* **1978**, *17*, 126.

Scheme 1. Pauson–Khand Reaction^a

^a See Figures 1 and 2 for 3D views of the title compound.

of a diamagnetic ground state of Co₂(CO)₈. Analysis of the theoretical energy density^{2d} locates a shallow minimum in $H(\mathbf{r})$ halfway between Co nuclei, interpreted as a bent Co–Co bond. The same authors use orbital-based arguments to demonstrate that core and nonbonding orbitals dominate the total electron density and, hence, that the energy density is a more sensitive probe of metal–metal bonding.^{2e} Very recently, Gatti analyzed a series of metal clusters, such as Mn₂(CO)₁₀ and Fe₂(CO)₉, as well as Co₂(CO)₈, in terms of the “source function”, that is, the contribution of all atoms in the system to the electron density at a given point.⁶ In this way, they showed that the density in the intermetallic region comes primarily from the oxygens of CO ligands rather than from the metals themselves, a somewhat counterintuitive finding that sheds fascinating new light on this long-standing problem.

A closely related class of compounds are alkyne-bridged dicobalt carbonyls, Co₂(CO)₆(C₂R₂). Early spectroscopic studies indicate a C_{2v} geometry, in which the alkyne lies perpendicular to the Co–Co direction.⁷ Orbital arguments again suggest a bent metal–metal bond, together with donation of electrons from filled π -orbitals on the alkyne into metal d-orbitals, along with back-donation into formally empty π^* -orbitals. Such complexes are of particular interest because of their role in the Pauson–Khand reaction, a widely used method for regioselective synthesis of cyclopentanones⁸ (see Scheme 1). Indeed, these bridged dicobalt species are the only intermediates isolated from typical reaction conditions. Complexes of this form are used as models for electronic communication along molecular wires, in which the Co₂C₂ core acts as a redox center capable of interacting with remote metal centers connected by a di-yne or poly-yne chain.⁹ Cobalt alkyne complexes have also recently been found to exhibit interesting antitumor properties and may be effective in the treatment of leukemia, although the exact biological target and mode of action remain unclear.¹⁰

Even in the simple MO picture defined by Thorn et al., the bonding and electronic structure in these complexes is open to interpretation: as discussed above, metal–metal bonding has been a particular focus. However, this is more than an academic question because the nature of Co–C

bonding and any donation/back-donation present will have an effect on the subsequent reactivity of the alkyne. Recently, density functional theory (DFT) methods have been used to propose intermediates and transition states on the Pauson–Khand reaction pathway.¹¹ Probing the electronic structure of metal poly-yne compounds is crucial to understanding their behavior and possible development for use in molecular devices.¹² However, the success or failure of such treatments rests on the appropriate choice of theoretical method, one capable of properly describing the bonding in bridged dicobalt complexes.

Computational Methodology

All ab initio calculations were carried out using the Gaussian03 suite of programs.¹³ The geometry was extracted from recent high-resolution X-ray results,¹⁴ with substituents on the alkyne bridge replaced with H, symmetry-independent Co–C_{alkyne} and Co–C_{CO} distances averaged, and the overall geometry symmetrized to the C_{2v} point group (see Supporting Information). The basis sets employed included Pople’s 6-31G and Wachters and Hay’s 6-311G¹⁵ all-electron split-valence sets on Co, augmented with a single-shell of f-functions with an exponent recommended by Ehlers et al.,¹⁶ as well as the Lanl2DZ basis set and effective core potential (ECP).¹⁷ Dunning’s correlation consistent cc-pVDZ and cc-pVTZ functions¹⁸ were placed on C, H, and O atoms. We note that these

- (6) Gatti, C.; Lasi, D. *Faraday Discuss.* **2007**, *135*, 55.
 (7) (a) Howard, J.; Robson, K.; Waddington, T. C. *Chem. Phys.* **1981**, *61*, 53. (b) Iwashita, Y.; Tamura, F.; Nakamura, A. *Inorg. Chem.* **1969**, *8*, 1179.
 (8) Geis, O.; Schmalz, H.-G. *Angew. Chem., Int. Ed.* **1998**, *37*, 911.
 (9) Low, P. J.; Rousseau, R.; Lam, P.; Udachin, K. A.; Enright, G. D.; Tse, J. S.; Wayner, D. D. M.; Carty, A. J. *Organometallics* **1999**, *18*, 3885.
 (10) Ott, I.; Kircher, B.; Gust, R. *J. Inorg. Biochem.* **2004**, *98*, 485–489.

- (11) Yamanaka, M.; Nakamura, E. *J. Am. Chem. Soc.* **2001**, *123*, 1703.
 (12) Koentjoro, O. F.; Rousseau, R.; Low, P. J. *Organometallics* **2001**, *20*, 4502.
 (13) Frisch, M. J.; Trucks, G. W.; Schlegel, H. B.; Scuseria, G. E.; Robb, M. A.; Cheeseman, J. R.; Montgomery, J. A., Jr.; Vreven, T.; Kudin, K. N.; Burant, J. C.; Millam, J. M.; Iyengar, S. S.; Tomasi, J.; Barone, V.; Mennucci, B.; Cossi, M.; Scalmani, G.; Rega, N.; Petersson, G. A.; Nakatsuji, H.; Hada, M.; Ehara, M.; Toyota, K.; Fukuda, R.; Hasegawa, J.; Ishida, M.; Nakajima, T.; Honda, Y.; Kitao, O.; Nakai, H.; Klene, M.; Li, X.; Knox, J. E.; Hratchian, H. P.; Cross, J. B.; Bakken, V.; Adamo, C.; Jaramillo, J.; Gomperts, R.; Stratmann, R. E.; Yazyev, O.; Austin, A. J.; Cammi, R.; Pomelli, C.; Ochterski, J. W.; Ayala, P. Y.; Morokuma, K.; Voth, G. A.; Salvador, P.; Dannenberg, J. J.; Zakrzewski, V. G.; Dapprich, S.; Daniels, A. D.; Strain, M. C.; Farkas, O.; Malick, D. K.; Rabuck, A. D.; Raghavachari, K.; Foresman, J. B.; Ortiz, J. V.; Cui, Q.; Baboul, A. G.; Clifford, S.; Cioslowski, J.; Stefanov, B. B.; Liu, G.; Liashenko, A.; Piskorz, P.; Komaromi, I.; Martin, R. L.; Fox, D. J.; Keith, T.; Al-Laham, M. A.; Peng, C. Y.; Nanayakkara, A.; Challacombe, M.; Gill, P. M. W.; Johnson, B.; Chen, W.; Wong, M. W.; Gonzalez, C.; Pople, J. A. *Gaussian 03*, revision C.02; Gaussian, Inc.: Wallingford, CT, 2004.
 (14) Overgaard, J. Unpublished data.
 (15) (a) Windus, T. L. *J. Chem. Phys.* **1998**, *109*, 1223. (b) Wachters, A. J. H. *J. Chem. Phys.* **1970**, *52*, 1033. (c) Hay, P. J. *J. Chem. Phys.* **1977**, *66*, 4377.
 (16) Ehlers, A. W.; Bohme, M.; Dapprich, S.; Gobbi, A.; Hillwarth, A.; Jonas, V.; Kohler, K. F.; Stegmann, R.; Veldkamp, A.; Frenking, G. *Chem. Phys. Lett.* **1993**, *208*, 111.
 (17) Hay, P. J.; Wadt, W. R. *J. Chem. Phys.* **1985**, *82*, 284.
 (18) Dunning, T. H., Jr. *J. Chem. Phys.* **1989**, *90*, 1007.

Table 1. Hartree–Fock and CAS-SCF Results with 6-31G(f)+cc-pVDZ Basis Set

multiplicity	job type	total energy (E_h)	relative energy ^a (eV)	S^2
1	RHF	-3515.33723	0.0	0.00
1	UHF	-3515.47449	-3.735	2.51
1	CAS[6,6]	-3515.53367	-5.345	0.00
1	CAS[22,14]	-3515.56143	-6.101	0.0
1	CAS[6,6]-PT2	-3519.13789		0.0
1	CAS[22,14]-PT2	-3519.08736		0.0
3	UHF	-3515.45700	-3.259	4.42
3	CAS[6,6]	-3515.48869	-4.121	2.00
3	CAS[22,14]	-3515.50971	-4.693	2.00
3	CAS[6,6]-PT2	-3519.06759		2.00
3	CAS[22,14]-PT2	-3519.00341		2.00
5	UHF	-3515.41030	-1.988	7.35
7	UHF	-3515.35958	-0.608	12.73
9	UHF	-3515.26963	+1.839	20.66

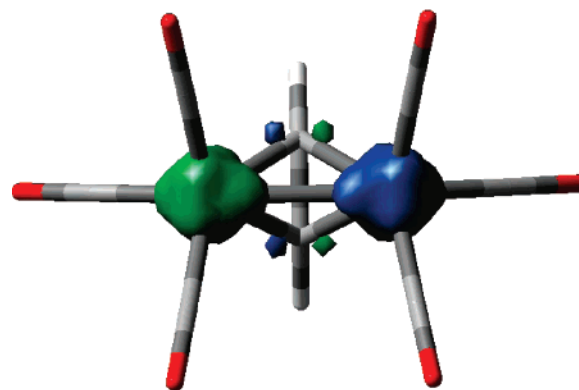
^a Relative to RHF singlet energy, 1 eV = 23.06 kcal mol⁻¹ = 96.49 kJ mol⁻¹. Values not reported for CAS-PT2 calculations since these are not strictly comparable to RHF/UHF.

are similar basis sets to those used recently by Kenny et al.¹⁹ and by Bachler et al.²⁰ in studies of cobalt carbonyl complexes and of singlet diradical Ni complexes, respectively. The stability of all Hartree–Fock wavefunctions was tested using the criteria of Seeger and Pople,²¹ and where applicable, lower-energy solutions were obtained by following the eigenvector corresponding to instability. CAS-SCF calculations used the natural orbitals obtained from UHF calculations as a starting point, with visual inspection confirming the relevance of these to Co–Co or Co–C bonding (see below for more details).

Topological analysis of the electronic density, $\rho(\mathbf{r})$, is based upon those points where the gradient of the density, $\nabla\rho(\mathbf{r})$, vanishes. Bond critical points (bcp's) are located where one curvature (in the internuclear direction) is positive and two (perpendicular to the bond direction) are negative. Properties evaluated at such points are widely used to characterize bonding interactions. For example, covalent interactions between “light atoms” typically have large $\rho(\mathbf{r})$ and negative $\nabla^2\rho(\mathbf{r})$, while noncovalent and metal–ligand interactions are found to have low $\rho(\mathbf{r})$ and positive $\nabla^2\rho(\mathbf{r})$.²² For metal complexes in particular, this simple analysis has been found to be inadequate, and the energy density, $H(\mathbf{r})$, has been shown to be a more sensitive probe: in regions of covalent bonding, potential energy dominates, and $H(\mathbf{r})$ is negative. All electron density analysis was carried out using the AIMPACK²³ and AIM2000²⁴ suites of programs, and bond orders were calculated using an in-house program, available from the authors on request.

Results and Discussion

Table 1 contains the energy of the HF and CAS-SCF solutions found using 6-31G(f) on Co and cc-pVDZ on remaining atoms. The initial restricted Hartree–Fock (RHF) calculation converged smoothly, but stability analysis indicated that a lower-energy UHF solution existed. The optimal

**Figure 1.** Spin density of UHF solution, plotted at 0.05 au isosurface.

UHF solution is almost 4 eV more stable than the RHF value but yields an expectation value of the S^2 operator of 2.51, that is, much higher than the expected value of 0 for a singlet state. Such a large value of S^2 indicates significant spin contamination from higher multiplicity states, such that the term “singlet” may not be appropriate here. UHF calculations on higher spin-states are reported in Table 1, revealing that the triplet is just 0.49 eV higher in energy than the UHF singlet, while the quintet, septet, and nonet states are rather less stable. However, these higher multiplicity states cannot be ignored, as evidenced by the large S^2 values for the triplet and quintet states (4.4 and 7.4), compared with the expected values of 2 and 6, respectively. Only in the septet and nonet states does S^2 approach the “correct” values.

To test whether these findings are not simply an artifact of the basis set employed, RHF and UHF singlet energies were calculated using larger and smaller basis sets: with a triple- ζ basis (6-311G(f) on Co, cc-pVTZ on C, H, and O), the UHF solution is 4.03 eV below the RHF, while with the Lanl2DZ basis and ECP, the difference is 3.92 eV, that is, values not greatly different from those in Table 1. We therefore proceed with the combination of 6-31G* on Co and cc-pVDZ on C, H, and O because more advanced theoretical methods are computationally tractable for this complex using this basis set.

As pointed out by Bachler et al.,²⁰ “the singlet diradical character of a molecule is large provided the symmetry-broken unrestricted solution for the electronic ground state is much lower in energy than the energy of the restricted singlet ground-state solution”. We therefore take these Hartree–Fock results as evidence of significant singlet diradical character in the title compound. The spin density of this UHF singlet is shown in Figure 1, revealing large spins concentrated in Co d-orbitals, with smaller contributions from alkyne C p-orbitals. Mulliken spin populations reveal values of ± 2.0 e on Co, and values no larger than 0.1 e on any other atom. Spin charges were also calculated using AIM methods (see below for more details), resulting in values of ± 1.9 e on the Co atoms, that is, in general agreement with the Mulliken data.

Clearly, there is substantial multireference character in this complex, such that the single-reference Hartree–Fock procedure is inadequate, as evidenced by the large spin contamination observed. Natural orbitals from the UHF

- (19) Kenny, J. P.; King, R. B.; Schaefer, H. F., III. *Inorg. Chem.* **2001**, *40*, 900.
 (20) Bachler, V.; Olbrich, G.; Neese, F.; Wieghardt, K. *Inorg. Chem.* **2002**, *41*, 4179.
 (21) Seeger, R.; Pople, J. A. *J. Chem. Phys.* **1977**, *66*, 3045.
 (22) Bader, R. F. W.; Essen, H. *J. Chem. Phys.* **1984**, *80*, 1943.
 (23) Biegler-König, F. W.; Bader, R. F. W.; Tang, T.-H.; *J. Comput. Chem.* **1982**, *3*, 317. These programs can be obtained from <http://www.chemistry.mcmaster.ca/aimpac>.
 (24) Biegler-König, F. W.; Schönbohm, J. *J. Comput. Chem.* **2002**, *23*, 1489.

singlet revealed six orbitals with populations significantly different from the restricted values of two and zero: three occupied natural orbitals were found with populations between 1.2 and 1.95, and a corresponding set of three unoccupied with populations between 0.05 and 0.8 was also found. Visual inspection shows that these orbitals come in pairs of bonding and antibonding combinations: the first pair, with occupations of 1.22 and 0.78, consists almost solely of the in-phase and out-of-phase combination of Co d_z^2 orbitals (where z corresponds to the Co–Co internuclear vector). The remaining two pairs of “active” natural orbitals combine Co d -orbitals with C_{alkyne} p -orbitals and have occupations of 1.79, 1.46, 0.54, and 0.21 electrons. Graphical representations of these natural orbitals can be found in Supporting Information.

Guided by these results, we then carried out CAS-SCF calculations on the singlet state, using several choices of active space based on the UHF natural orbitals. The first included only the bonding/antibonding d_z^2 orbitals, denoted CAS[2,2], and the second contained all six natural orbitals with significant noninteger values, denoted CAS[6,6]. The CAS[2,2] calculation suffered severe convergence problems, perhaps indicative of too severe an imbalance between active and inactive spaces. Despite repeated attempts with various convergence options, no stable CAS[2,2] solution could be found; these calculations were therefore not pursued any further.

In contrast, CAS[6,6] converged smoothly from the UHF guess to a solution with occupation numbers of active orbitals equal to 1.88, 1.80, 1.67, 0.33, 0.19, and 0.12 electrons, that is, substantially closer to restricted values of 2.0 and 0.0 than the starting point. This overestimation of biradical character by UHF methods is well-known.²⁵ These orbitals are shown in Figure 2. Visual inspection of these CAS[6,6] orbitals reveals that the pair with largest deviation from integer occupations, a and b in Figure 2, are indeed the Co–Co bonding/antibonding pair of d_z^2 -orbitals on Co. The remaining two pairs consist of in-phase/out-of-phase combinations of Co d -orbitals with π^* orbitals on the alkyne. This CAS[6,6] expansion is dominated by two configuration state functions (CSFs), namely, the original RHF state (with coefficient 0.85) and the biradical state (0.33), with all other CSFs contributing less. Full details are given in Supporting Information.

The CAS[6,6] energy is 1.6 eV lower than that of the singlet UHF solution and more than 5 eV below the original RHF value, showing that substantial stabilization results from the greater flexibility of these CAS calculations. Although natural orbital occupation numbers can give a guide to choosing an active space, this does not permit an assessment of convergence with respect to active space. We therefore carried out further CAS calculations, including *all* metal d -orbitals, C–C π - and π^* -orbitals, along with the three “virtual” orbitals from the CAS[6,6] treatment (the [6,6] active space is therefore a subset of this [22,14] one). In total, this forms a CAS[22,14] calculation, consisting of over 40 000 possible configurations. This also converged smoothly,

and Table 1 shows that this treatment lowers the energy of the singlet state by a further 0.7 eV. Weights of CSFs are similar to the CAS[6,6] results given above, with just two CSFs dominating.

The data presented in Table 1 indicates that the ground state is a singlet diradical or, equivalently, that there is weak antiferromagnetic coupling between cobalt atoms in this complex. For such diradical species, the key spectroscopic parameter of interest is the energy splitting between singlet and triplet states, identified with the J coupling constant used in spin Hamiltonian methods and experimentally determined by magnetic susceptibility or heat capacity curves.²⁶ We have therefore carried out corresponding CAS calculations on the triplet state using both [6,6] and [22,14] active spaces, based on the natural orbitals from the UHF singlet calculation. Table 1 reports triplet energies from UHF, as well as CAS-[6,6] and -[22,14] calculations, from which we estimate singlet–triplet energy splittings of 0.47, 1.22 and 1.40 eV, respectively. Thus, CAS results yield a much larger singlet–triplet gap than does UHF, further evidence for the overestimation of singlet biradical character by the latter. The two choices of active space give similar results, although one could not claim that the result is converged with the smaller active space. Nonetheless, we believe the results are sufficiently close to use CAS[6,6] wavefunctions to analyze electron density and bonding.

While CAS-SCF calculations properly describe the multireference character of such systems, the small active space that must necessarily be employed means that dynamic correlation is largely neglected. We have therefore calculated the second-order perturbation theory correction to the CAS energies for singlet and triplet states, denoted CAS-PT2 in Table 1. The inclusion of dynamic correlation dramatically lowers the energy of each state, and lowers that of the singlet more than that of the triplet, such that these data further increase the singlet–triplet energy gap to 1.913 and 2.284 eV, using small and large active spaces, respectively. These singlet–triplet energy gaps reported in Table 1 are much larger than those reported for the archetypal diradical copper complexes discussed by Moreira and Illas,²⁶ where typical values range from 10 to 100 meV.

DFT is a computationally attractive procedure for treatment of singlet diradical species, applicable to larger species than the *ab initio* treatment described above. Despite the theoretical basis of this approach having been questioned by some authors, numerous studies show that hybrid functionals are capable of yielding at least a qualitatively correct description of bonding and J couplings.^{26,27} Calculations employing two different hybrid functionals, that is, B3LYP and mPW1PW91, showed the same restricted to unrestricted instability seen for HF data above. However, in these cases, the energy difference between these solutions is much smaller, with values of 0.007 and 0.07 eV, respectively. These functionals differ markedly in their description of the unrestricted ground state, for example, yielding Mulliken spin

(25) Jensen, F. *Introduction to Computational Chemistry*, 2nd ed.; Wiley: Chichester, U.K., 2006.

(26) Moreira, I. P. R.; Illas, F. *Phys. Chem. Chem. Phys.* **2006**, *8*, 1645.
(27) Cramer, C. J.; Welch, M.; Piecuch, P.; Puzarini, C.; Gagliardi, L. *J. Phys. Chem. A* **2006**, *110*, 1991.

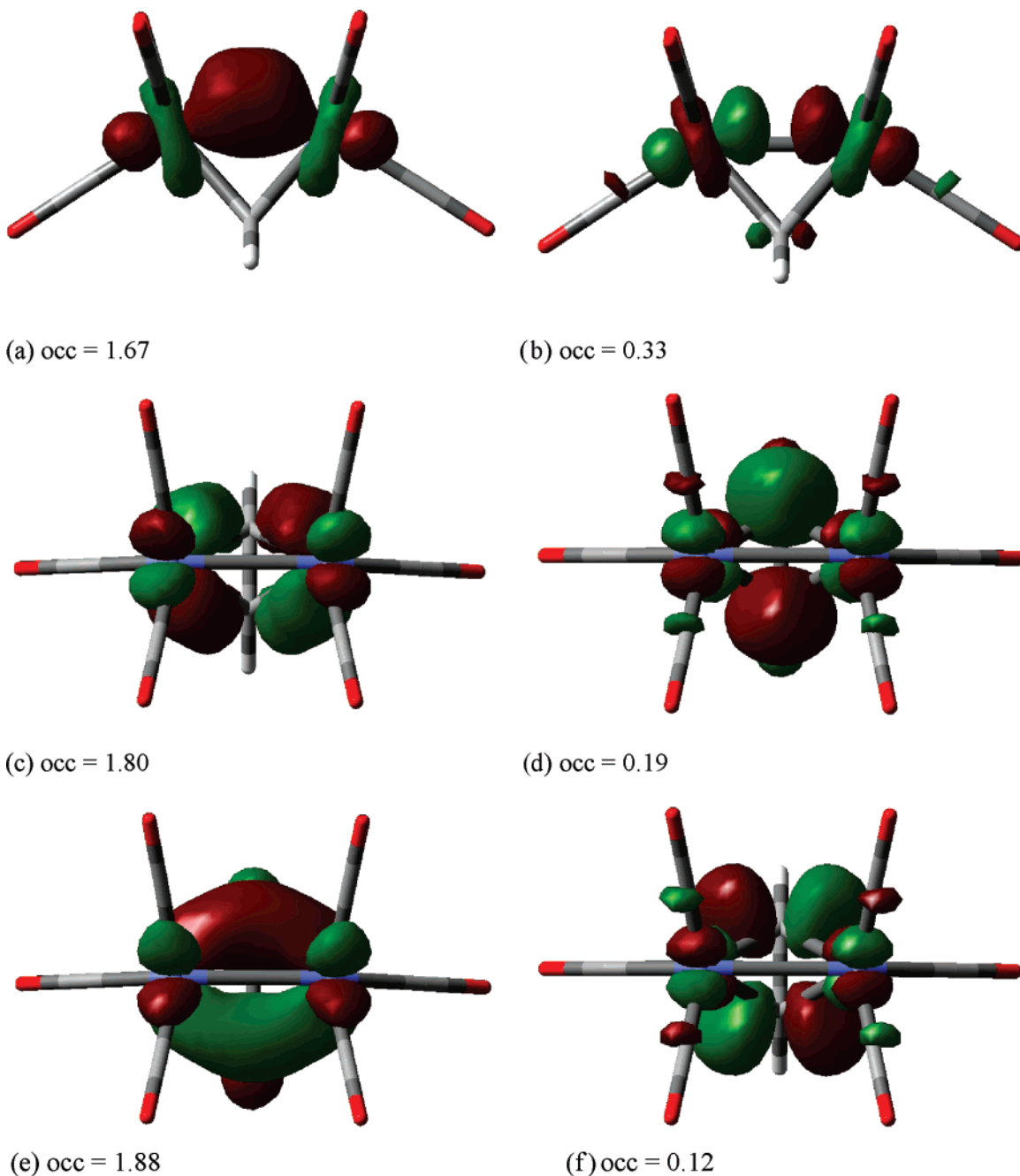


Figure 2. Six active orbitals from CAS[6,6], plotted with isosurface value of 0.05 au.

charges on each Co of ± 0.41 and ± 0.71 e, respectively. Despite these differences, hybrid DFT values for singlet–triplet splitting are in reasonable agreement with ab initio values at 1.37 and 1.20 eV, respectively.

In contrast, two pure DFT methods, BLYP and PBEPBE, lead to stable restricted solutions and no unrestricted ground state. While this seems at odds with the ab initio data presented above, these functionals yield singlet–triplet splitting values of 2.07 and 2.09 eV, respectively, that is, rather higher than those from hybrid DFT methods but much closer to the best ab initio value from CAS-PT2 calculations. This is similar to the findings of Cramer et al., who showed that pure DFT methods outperform hybrid ones in prediction of the relative energies of Cu_2O_2 isomers.²⁷ This could be interpreted as evidence that the nondynamical correlation is

well accounted for in the pure functional, while incorporation of HF exchange via the hybrid functional introduces UHF character, as discussed by Cramer et al. In the absence of experimental confirmation of this spectroscopic quantity, it is difficult to reach a sure conclusion on this matter from these data.

The occupation of bonding and antibonding orbitals in the CAS[6,6] wavefunction suggests a rather more complex picture of metal–metal and metal–ligand bonding than might be initially inferred. QTAIM analysis on the ground-state singlet CAS[6,6] electron density was employed to gain deeper insight into the bonding. The first and most obvious result from this is the lack of a bond critical point (bcp) in the region between cobalt nuclei, despite exhaustive searching of the internuclear region. Four Co–C_{alkyne} bonds are

Table 2. Topological Analysis of Electron Density (au)^a

bond	ρ	$\nabla^2\rho$	λ_1	λ_2	λ_3	G	V	H
Co–C _{alkyne}	0.104	+0.223	−0.114	−0.059	+0.397	0.106	−0.156	−0.050
	0.102	+0.207	−0.116	−0.070	+0.392	0.096	−0.141	−0.045
C–C	0.318	−0.739	−0.544	−0.491	+0.296	0.140	−0.465	−0.325
	0.318	−0.686	−0.535	−0.526	+0.375	0.142	−0.455	−0.313
Co–C _{CO} 1	0.139	+0.763	−0.153	−0.127	+1.043	0.238	−0.286	−0.048
	0.144	+0.607	−0.162	−0.160	+0.929	0.202	−0.252	−0.050
Co–C _{CO} 2	0.131	+0.711	−0.135	−0.123	+0.969	0.222	−0.267	−0.045
	0.135	+0.571	−0.155	−0.148	+0.875	0.190	−0.237	−0.047

^a Reported as CAS[6,6] on first line and BLYP on the second. Properties at bond critical points: ρ = total electron density; $\nabla^2\rho$ = Laplacian of electron density; $\lambda_1, \lambda_2, \lambda_3$ = curvatures of electron density; G = kinetic energy density; V = potential energy density; H = total energy density.

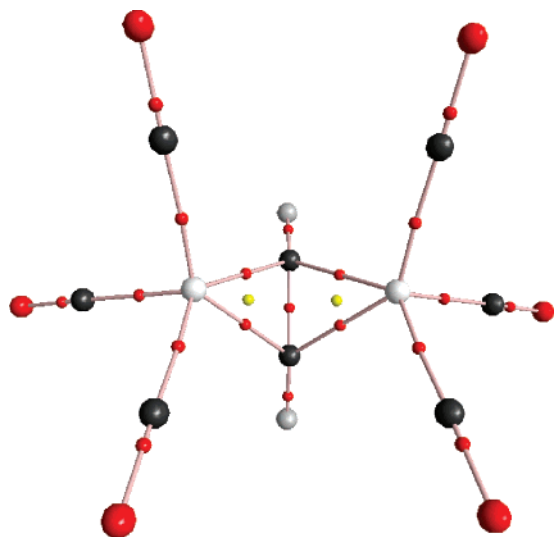


Figure 3. Molecular graph of **1** resulting from CAS[6,6] wavefunction. Bond critical points shown as red dots, and ring critical points are shown as yellow dots.

present in this analysis, along with all expected Co–C_{CO}, C–C, C–O, and C–H bcp's. Properties of selected critical points are reported in Table 2, and the resulting molecular graph created from the theoretical results is displayed in Figure 3, indicating the presence of two 3-membered metallocycles in the Co₂C₂ core, sometimes referred to as a “butterfly arrangement”.

Electron density data suggests substantial overlap between the cobalt and coordinated alkyne: values of $\rho(r)$ are low, and $\nabla^2\rho(r)$ values are positive in all cases, as is normal for metal–ligand bonds. The energy density at the bcp is dominated by the potential energy, leading to a value less than zero in all bonds, indicative of significant covalent bonding. Cobalt–carbonyl bonds show the properties expected on the basis of previous work, with low $\rho(r)$ and positive $\nabla^2\rho(r)$ values. The value of $\rho(r)$ at the bcp has long been used as a measure of bond order, especially, in nonpolar bonds such as C–C. The value of $\rho(r)$ in the bridging alkyne is rather low: for comparison, ethane has a value of 0.249, ethene 0.352, and ethyne 0.403 au, from RHF calculations²⁸ with the same basis set, suggesting the alkyne might be better described as having a bond order of between 1.5 and 2.0.

In the light of the apparent success of pure DFT methods in reproducing ab initio data for spectroscopy discussed

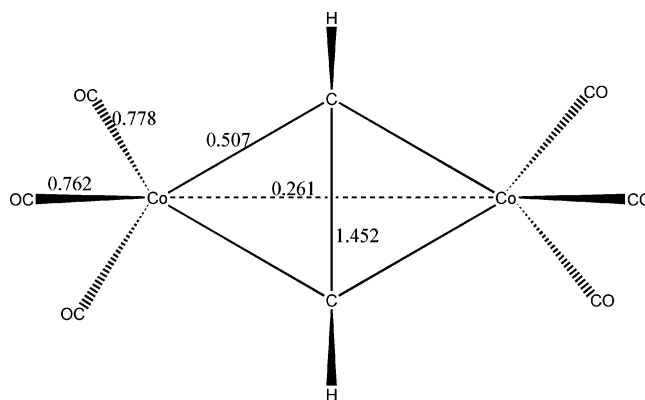


Figure 4. $\delta(A,B)$ bond orders for metal–metal and metal–ligand interactions.

above, we also carried out AIM analysis of the BLYP-calculated electron density. Because this DFT density should include the effects of electron correlation for the whole molecule, one might expect this to give a more balanced picture of the bonding. In fact, very little difference is observed between CAS[6,6] and BLYP density. The molecular graph that results is essentially identical to that shown in Figure 3, with no Co–Co bcp and four Co–C_{alkyne} bcp's, and it is shown in Supporting Information. Table 2 reports BLYP properties at these bond critical points, which again show only small differences from the CAS[6,6] data, especially within the Co₂C₂ core. Slightly larger changes are seen for the Co–C_{CO} bonds, which is unsurprising since these bonds are not included in the CAS[6,6] active space. At this BLYP level, ethane, ethene, and ethyne have ρ_{bcp} values equal to 0.240, 0.345, and 0.404 au, respectively, such that the alkane again appears to lie between ethane and ethene.

As discussed above, the use of the electron density alone in unambiguously identifying bonding interactions in transition metal systems has been questioned: we therefore turn to two alternative metrics, the energy density, $H(\mathbf{r})$, and the atomic overlap matrix (AOM). The AOM is derived from the electron-pair distribution function $\rho(\mathbf{r}_1, \mathbf{r}_2)$ integrated over atomic basins defined by QTAIM. Definitions of atomic localization $\delta(A,A)$ and delocalization $\delta(A,B)$ have been set out from this, the latter leading to robust definitions of bond order, even for atoms that do not share a common interatomic surface.²⁹ Macchi et al. have employed $\delta(A,B)$ from Hartree–Fock calculations to explore metal–metal bonding in

(28) RHF calculations are used as a reference since the σ and π -orbitals of the alkyne are not included in the CAS[6,6] active space and, hence, are not correlated with Co d-orbitals or C–C σ^* - and π^* -orbitals.

(29) (a) Bader, R. F. W.; Stephens, M. E. *J. Am. Chem. Soc.* **1975**, *97*, 7391. (b) Angyan, J. G.; Loos, M.; Mayer, I. *J. Phys. Chem.* **1994**, *98*, 5244.

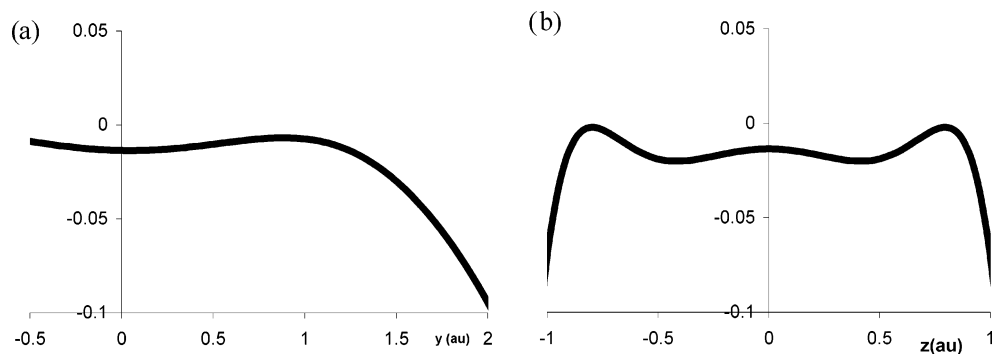


Figure 5. Energy density from CAS[6,6] wavefunction along (a) 2-fold (y) axis and (b) parallel to the Co–Co (z) axis (au).

a range of compounds, quoting a value of 0.37 between Co atoms in $\text{Co}_2(\text{CO})_8$, where a value of 1.0 indicates a single bond.³⁰ We calculate a value for $\delta(\text{Co},\text{Co})$ of 0.26 from the CAS[6,6] wavefunction, although direct comparison of these numbers is not possible because of the different theoretical methods employed. Thus, the atomic overlap data suggests a weak but nonzero overlap between cobalt atoms, in complete agreement with the structural and orbital arguments presented above.

$\delta(\text{A},\text{B})$ values for Co–C and C–C bonds have also been calculated, and are shown in Figure 4. This shows substantial covalent character of all C–C bonds (for comparison, Macchi et al. report values of 0.70 for the bridging Co–C bonds in $\text{Co}_2(\text{CO})_8$). The value of 1.45 for the alkyne C–C bond suggests that it has been considerably weakened by coordination to two cobalts, such that little of the π -overlap between carbon atoms remains. This agrees with conclusions drawn from the ρ_{bcp} alone and also with the picture gleaned from inspection of the active orbitals in Figure 2, which shown donation from metal d-orbitals into π^* -orbitals on the alkyne.

The energy density, $H(\mathbf{r})$, is a popular alternative to $\rho(\mathbf{r})$ for probing bonding interactions in complexes such as this. Finger et al.^{24,e} plotted this function along the 2-fold axis of $\text{Co}_2(\text{CO})_8$, using restricted B3LYP methods, finding a clear minimum close to the intersection of the 2-fold axis and the Co–Co vector, which they interpret as evidence for bent metal–metal bonding. Figure 5 shows plots of $H(\mathbf{r})$ along both the 2-fold (y) axis and the perpendicular Co–Co (z) axis.³¹ Along the 2-fold axis, $H(\mathbf{r})$ shows some similarities to the plots reported by Finger et al.,^{24,e} with a shallow minimum close to the Co–Co vector (Co atoms are located at $y = +0.141 \text{ \AA}$).³² In the perpendicular direction, large negative values are found close to the Co nuclei, rising close to $H(\mathbf{r}) = 0$ at $z = \pm 0.41 \text{ \AA}$. Minima are observed at $z = \pm 0.21 \text{ \AA}$, but at $z = 0$, we find that $H(\mathbf{r})$ is actually a maximum in this direction, such that we cannot assign this

point as a local minimum in $H(\mathbf{r})$, but instead it is a saddle point. Nonetheless, it is clear from these plots that $H(\mathbf{r})$ has a negative value throughout the region between cobalt nuclei, again supporting the picture of some covalent overlap between metals obtained from $\delta(\text{A},\text{B})$ values.

A further diagnostic tool of bonding interactions based on energy densities has been proposed by Espinosa³³ and used in several works to probe bonding in metal–carbonyl clusters.^{1e,6,34} In this, the ratio of potential to kinetic energy densities, $|V(\mathbf{r})|/G(\mathbf{r})$, is calculated at bond critical points. A value of greater than two taken as indicative of shared or covalent interaction, while a value of less than one indicates closed-shell interaction. Between these extremes, a “transit” region of incipient covalent bonding is proposed. Using the CAS[6,6] wavefunction, we calculate values for this ratio of 1.34 at the midpoint of the Co–Co vector and 1.44 at the saddle point in $H(\mathbf{r})$ identified above, that is, both within the transit region, consistent with the other results that point to some covalent character in the metal–metal region. Gatti et al. used similar diagnostics to compare bridged and unbridged forms of $\text{Co}_2(\text{CO})_8$, in which they found $|V|/G$ to be a useful tool to distinguish these binding modes, and they reported similar values to those reported above (notwithstanding differences in theoretical methods employed).⁶

In addition to bonding interactions, QTAIM defines a rigorous partition of real space into atomic basins, used to calculate properties of individual atoms within molecules. This definition yields an atomic charge of +0.669 e on each Co and of –0.408 on each alkyne C, consistent with the picture of donation of electrons from a formal $\text{Co}^{(0)}$ into π^* -orbitals on the alkyne. Natural population analysis (NPA) yields a similar picture of charges, with +0.813 on each Co and –0.814 on each alkyne C, stemming from a $3d^{7.69}4s^{0.44}4p^{0.04}$ configuration on Co. Further correspondence between the NBO and QTAIM interpretations of bonding stems from the absence of a bonding Co–Co orbital in the NBO analysis.

Conclusions

Ab initio and DFT calculations indicate that the ground-state electronic structure of the alkyne-bridged dicobalt complex $\text{Co}_2 \mu\text{-C}_2\text{H}_2 (\text{CO})_6$ is best described as a singlet

(30) Macchi, P.; Sironi, A. *Coord. Chem. Rev.* **2003**, 383, 238.

(31) Figure 5b is not directly along the Co–Co vector but is parallel to it at the y -coordinate (+0.078) for which a minimum in $H(\mathbf{r})$ is suggested by the former. Thus, the full Cartesian coordinates (in au) used to generate Figure 5a are (0.0, –0.5, 0.0) to (0.0, 2.0, 0.0), and those used to generate Figure 5b are (0.0, 0.078, –1.0) to (0.0, 0.078, 1.0).

(32) The fact that the 2-fold axis also bisects the C–C bond means that this function reaches a large negative value at higher values of y (C’s are located at $y = +2.941 \text{ au}$), unlike in the case of $\text{Co}_2(\text{CO})_8$. In the x -direction, $H(\mathbf{r})$ reaches a minimum at the intersection with the directions plotted in Figure 5.

(33) Espinosa, E.; Alkorta, I.; Elguero, J.; Molins, E. *J. Chem. Phys.* **2002**, 117, 5529.

(34) Farrugia, L. J.; Mallinson, P. R.; Stewart, B. *Acta Crystallogr., Sect. B* **2003**, B59, 234.

diradical, with partial occupation of both bonding and antibonding orbitals between Co atoms. This is evident in Hartree–Fock, CAS-SCF, and hybrid DFT calculations, although pure DFT methods are at odds with these findings. These methods indicate that the singlet ground state is between 1.2 and 1.9 eV lower in energy than the lowest triplet state, that is, a considerably larger energy splitting than in archetypal diradical species such as $[\text{Cu}_2\text{Cl}_6]^{2-}$. Topological analysis of the CAS-SCF electron density suggests the absence of a direct Co–Co bond, but other indicators such as the atomic overlap matrix and the total energy density reveal significant overlap between cobalt atomic basins, contributing to the stabilization of the complex. These results suggest that caution should be exercised in the selection of theoretical methods for study

of such complexes, for example, in proposing and testing mechanisms for the Pauson–Khand reaction or their use as models for molecular devices.

Acknowledgment. The authors are grateful to referees for their detailed and insightful comments on this manuscript. All calculations were carried out on Cardiff University's Helix computational facility (www.helix.cf.ac.uk).

Supporting Information Available: Cartesian coordinates employed, graphical representations of natural orbitals from UHF calculations, details of CAS-SCF and CAS-PT2 calculations, and AIM analysis of the BLYP density. This material is available free of charge via the Internet at <http://pubs.acs.org>.

IC070278T